Robotic Grasp Initiation by Gaze Independent Brain-controlled Selection of Virtual Reality Objects

Christoph Reichert[1,2], Matthias Kennel[3], Rudolf Kruse[2], Hans-Jochen Heinze[1,4,5], Ulrich Schmucker[3], Hermann Hinrichs[1,4,5] and Jochem W. Rieger[6]

[1]*Department of Neurology, University Medical Center A.ö.R., D-39120, Magdeburg, Germany*
[2]*Department of Knowledge and Language Processing, Otto-von-Guericke University, D-39106, Magdeburg, Germany*
[3]*Fraunhofer Institute for Factory Operation and Automation IFF, D-39106, Magdeburg, Germany*
[4]*Leibniz Institute for Neurobiology, D-39118, Magdeburg, Germany*
[5]*German Center for Neurodegenerative Diseases (DZNE), D-39120, Magdeburg, Germany*
[6]*Department of Applied Neurocognitive Psychology, Carl-von-Ossietzky University, D-26111, Oldenburg, Germany*

Keywords: BCI, P300, Oddball Paradigm, Grasping, MEG.

Abstract: Assistive devices controlled by human brain activity could help severely paralyzed patients to perform everyday tasks such as reaching and grasping objects. However, the continuous control of anthropomorphic prostheses requires control of a large number of degrees of freedom which is challenging with the currently achievable information transfer rate of noninvasive Brain-Computer Interfaces (BCI). In this work we present an autonomous grasping system that allows grasping of natural objects even with the very low information transfer rates obtained in noninvasive BCIs. The grasp of one out of several objects is initiated by decoded voluntary brain wave modulations. A universal online grasp planning algorithm was developed that grasps the object selected by the user in a virtual reality environment. Our results with subjects demonstrate that training effort required to control the system is very low (<10 min) and that the decoding accuracy increases over time. We also found that the system works most reliably when subjects freely select objects and receive virtual grasp feedback.

1 INTRODUCTION

Brain-Computer Interfaces (BCI) translate human brain activity to machine commands (Wolpaw, 2013) and are in the focus of research to replace motor functions of severely paralyzed patients. In these patients, peripheral nerves do not provide any signal, like the electromyogram (EMG), to control prostheses (Kuzborskij et al., 2012). In the recent years, highly invasive techniques were tested to control prosthetic devices by voluntary modulation of brain activity (Hochberg et al., 2012; Velliste et al., 2008). In humans, the use of noninvasive techniques, like the electroencephalogram (EEG), is preferable over invasive recordings. Recently, it has been shown that a large number of hand movements can be discriminated with noninvasive EMG (Kuzborskij et al., 2012). However, only a small number of commands can be discriminated with noninvasively assessed motor imagery and, as a consequence, these systems do not allow for full control of complex manipulators with many degrees of freedom. Here we report progress in our development of a noninvasive BCI that enables users to grasp natural objects. Our approach combines the development of both efficient brain decoding techniques and autonomous actuator control to overcome the limited information transfer from noninvasive BCIs.

Commonly, movement commands are generated by motor imagery tasks aiming to decode the μ-rhythm (Pfurtscheller et al., 2000). However, a considerable percentage of people are unable to control motor imagery BCIs (Guger et al., 2003; Vidaurre and Blankertz, 2010). In contrast, it was shown that a larger fraction of people is able to select items in speller paradigms using an oddball task (Guger et al., 2009). The matrix speller was first

Reichert C., Kennel M., Kruse R., Heinze H., Schmucker U., Hinrichs H. and W. Rieger J..
Robotic Grasp Initiation by Gaze Independent Brain-controlled Selection of Virtual Reality Objects.
DOI: 10.5220/0004608800050012
In *Proceedings of the International Congress on Neurotechnology, Electronics and Informatics* (NEUROTECHNIX-2013), pages 5-12
ISBN: 978-989-8565-80-8

introduced by Farwell and Donchin (1988). In the oddball task a P300, a positive EEG deflection, is evoked when a rare target stimulus appears in a series of irrelevant stimuli. While it is often assumed that the accuracy of visually stimulated P300 speller is independent of gaze direction, it has recently been shown that the performance of the matrix speller drops significantly if the eyes are *not* moved toward the target (Brunner et al., 2010). The reason is that two EEG components, the P300 and the N200, contribute information when the centre of regard is moved to the target (Frenzel et al., 2011), whereas only the P300 is present if the eyes don't move. This could render the P300 paradigm less useful for patients who cannot move their eyes.

In this work we demonstrate that the visual oddball paradigm can be successful applied to initiate targeted grasps in a visually complex virtual environment with multiple realistic objects. Importantly, we show that the paradigm developed here works independent of the user's ability to direct gaze towards the target object. This is of high relevance for the targeted user group.

The other approach in our strategy for the development of a brain controlled robotic manipulator is to implement an algorithm to provide intelligent autonomous manipulation of predefined objects. Here we propose a new analytical grasp planning algorithm to achieve autonomous grasping of arbitrary objects. In contrast to other motion planning algorithms, our algorithm is not based on Learning by Demonstration (for a review see Sahbani, El-Khoury and Bidaud (2012)) and involves, but is not limited to, the robot's kinematics.

2 MATERIALS AND METHODS

In this study we decoded in real-time the magnetoencephalogram (MEG) of 17 subjects (9 male, 8 female, mean age 26.6) to determine their intention to select one of six selectable realistic objects for grasping. We used the decoding results to initiate a grasp of a robotic gripper. All subjects gave written informed consent. The study was approved by the ethics committee of the Medical Faculty of the Otto-von-Guericke University of Magdeburg.

2.1 Virtual Environment

We presented six objects (see Figure 1) placed at fixed positions in a virtual reality environment. The visual angle between outmost left and right objects was 8.5°. We defined circular regions on the table which were used i) to stimulate the subjects with visual events by lighting up the object background and ii) to provide cues and feedback by colouring the region's shape. A photo transistor placed on the screen was used to synchronize the ongoing MEG with the events displayed on the screen. To provide realistic feedback, the model of a robot (Mitsubishi RV E2) equipped with a three finger gripper (Schunk SDH) was part of the scene. The virtual robot is designed to mimic actual movements of the real robot. Specifically, an autonomously calculated grasp to the selected object is visualized.

Figure 1: VR scenario used for visual stimulation. This snapshot shows one flash event of an object.

2.2 Paradigm

The paradigm we employed is based on the P300 potential which is evoked approximately 300 ms after a rare target stimulus occurs in a series of irrelevant stimuli (oddball paradigm). In our variant of the paradigm, we marked objects by flashing their background for 100 ms. Objects were marked in random order with an interstimulus interval of 300 ms. Each object was marked five times per selection trial resulting in a stimulation interval length of 10 seconds.

Subjects were instructed to fixate the black cross centred to the objects and to count how often the target object was marked. The counting ensured that attention was maintained on the stimulus stream. In addition, subjects were instructed to avoid eye movements and blinking during the stimulation interval.

Each subject performed a minimum of seven runs with 18 selection trials per run. The runs were performed in three different modes that served different purposes. The number of runs each subject performed in each mode is listed in Table 1. We

started with the *instructed selection* mode. In this mode, the target object was cued by a light grey circle at the beginning of a trial and subjects were instructed to attend the cued object. Instructed selection was used in the initial training runs in which we collected data to train the classifier. In this mode true classifier labels are available which are required to train the classifier. We provided random feedback during training runs because no classifier was available in these initial runs. After the training runs, each subject performed several instructed runs with feedback. We denoted the second selection mode *free selection*. In this mode, subjects were free to choose the target object. In instructed selection mode and in free selection mode, a green circle was presented at the end of the trial on the decoded object as feedback. All other objects were marked by red circles. Free selection runs were performed after the instructed selection runs. In the third mode, the *grasp selection* mode, the virtual robot grasped and lifted the decoded target for feedback. Grasp selection runs were performed after free selection runs. In both modes, the free selection and grasp selection mode, the subject said "no" to signal that the classifier decoded the wrong object and remained silent otherwise.

Table 1: Number of runs the subjects performed in different selection modes.

Subject #	instructed		free	grasp
	training	decoder		
1	2	5	-	-
2	4	4	1	-
3	3	4	-	-
4-6	3	4	1	1
7	2	4	2	1
8	3	3	2	1
9	2	4	2	1
10	2	4	2	-
11	2	4	2	1
12	2	5	2	-
13-17	2	4	2	1

The results reported in this paper arise from online experiments. We did not exclude early sessions, causing slight changes in the experimental protocol during the study (Table 1). The number of runs performed in the different modes depended on cross validated classifier performance estimation and the development of detection accuracy. In total, five subjects performed three, one subject four and the remaining 11 subjects two initial training runs. Two subjects performed only instructed selections. Twelve of the subjects performed one run in the grasp selection mode. Here, only six instead of 18 trials were performed, due to the longer feedback duration.

2.3 Data Acquisition and Processing

The MEG was recorded with a whole-head BTi Magnes 248-sensors system (4D-Neuroimaging, San Diego, CA, USA) at a sampling rate of 678.17 Hz. Simultaneously, the electrooculogram (EOG) was recorded for subsequent inspection of eye movements. MEG data and event channels were instantaneously forwarded to a second workstation capable of processing the data in real-time. The data stream was cut into intervals including only the stimulation sequence. The MEG data were then band-pass filtered between 1 Hz and 12 Hz and down sampled to 32 Hz sampling rate. Then, the stimulation interval was cut in overlapping 1000 ms segments starting at each flash event. In instructed selection mode, the segments were labelled as target or nontarget segments depending on whether the target or a nontarget object was marked.

We used a linear support vector machine (SVM) as classifier because it provided reliably high performance in single trial MEG discrimination (Quandt et al., 2012; Rieger et al., 2008). These previous studies showed that linear SVM is capable of selecting appropriate features in high dimensional MEG feature spaces. We performed classification in the time domain, meaning that we used the magnetic flux measured in 32 time steps as classifier input. To reduce the dimensionality of the feature space, we empirically excluded 96 sensors located farthest from the vertex (the midline sensor at the position halfway between inion and nasion) which is the expected site of the P300 response. We further reduced the number of sensors by selecting the 64 sensors providing the highest sum of weights per channel in an initial SVM training on all preselected 152 sensors of the training run data. The selected feature set (64 sensors × 32 samples = 2048 features) was then used to train the classifier again and retrain the classifier after each run conducted in instructed selection mode.

2.4 Grasping Algorithm

In this section we describe the general procedure of our grasp planning algorithm, whereas we present the mathematical details in the Appendix. The algorithm was developed to physically drive a robot arm, but in this experiment it was used to provide virtual reality feedback. Importantly, in this strategy the robot serves as an intelligent, autonomous

actuator and does not drive predefined trajectories. The algorithm assumes that object position and shape coordinates relative to the manipulator are known to the system. In this experiment, coordinates of CAD-modelled objects were used. However, coordinates could as well be generated by a 3D object recognition system.

Central to our approach is that the contact surfaces of the gripper's fingers and the surfaces of the objects were rasterized with virtual point poles. We assumed an imaginary force field between the poles on the manipulator and the poles on the target object (see Appendix for details). The goal of the algorithm is to initially generate a manipulator posture that ensures a force closure grasp. The following grasp is organized by closing the hand in a real world scenario and by locking the object coordinates relative to the finger surface coordinates in the virtual scenario.

3 RESULTS

3.1 Decoder Accuracy

We determined the decoding accuracy as the ratio of correctly decoded objects divided by the total number of object selections. All subjects performed the task reliably above guessing level which was 16.7 %. On average, the intended object selections were correctly decoded from the MEG data in 77.7 % of all trials performed. Single subject accuracies ranged from 55.6 % to 92.1 %. In the instructed selection mode the average accuracy was 73.9 % and 85.9 % in the free selection mode. This performance difference is statistically significant (Wilcoxon rank sum test: p=0.03). When subjects received feedback by moving the virtual robot to the grasp target, the average accuracy was even higher and reached 91.2 %. Figure 2 depicts the evolution of decoding accuracies over runs. The height of the bars indicates the number of subjects (y-axis) who achieved the respective decoding performance out of 19 possible percentage bins. Each histogram shows the results from one run and the performance bins are equally spaced from 0 % to 100 %. The histograms are chronologically ordered from top to bottom. Yellow bars indicate results from instructed selection runs, blue bars indicate free selection run results and light red bars indicate results in runs with grasp feedback. Vertical dashed lines indicate the guessing level and thick solid lines indicate the average decoding accuracies over subjects (standard error marked grey). The average decoding accuracy increases gradually over the course of the experiment. Moreover, the histograms show that the highest accuracy over subjects was achieved in free selection runs. Note that our system achieved perfect detection in eight of the twelve subjects who received virtual grasp feedback. However, only six selections were performed by each subject in these grasp selection runs.

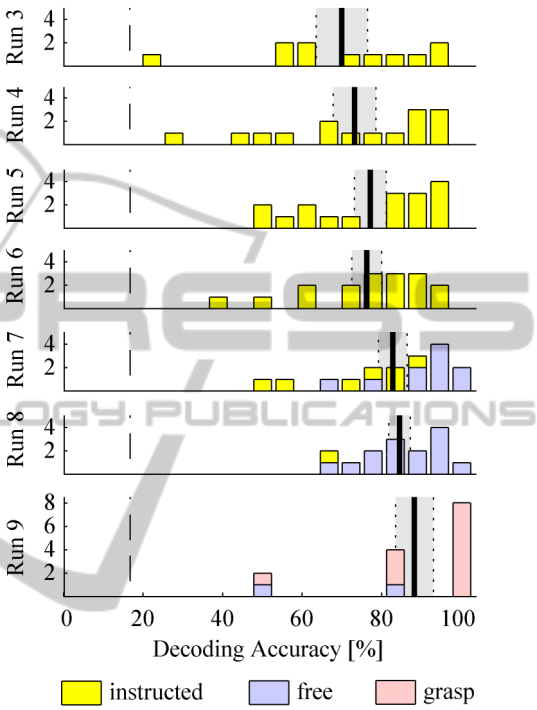

Figure 2: Performance histograms. The ordinate indicates the number of subjects who achieved a certain decoding accuracy. The histograms show data from different runs and code the type of run by colour. See text for details.

An established measure for the comparison of BCIs is the information transfer rate (ITR) which combines decoding accuracy and number of alternatives to a unique measure. We calculated the ITR according to the method of Wolpaw et al. (2000) at 3.4 to 12.0 bit/min for single subjects and 8.1 bit/min on average. Note that the maximum achievable bit rate with the applied stimulation scheme is 15.5 bit/min.

For online eye movement control, we observed the subjects' eyes on a video screen. In addition, we inspected the EOG measurements offline. Both methods confirmed that subjects followed the instruction to keep fixation.

3.2 Grasping Performance

We evaluated the execution duration of the online grasp calculation for different setups and objects. We implemented our grasping algorithm with the ability to distribute force computations to several parallel threads. Here, we permitted five threads employing a 2.8 GHz AMD Opteron 8220 SE processor. We calculated grasps of the six objects shown in Figure 1. To assess effects of object position, we arranged the objects at different positions within the limits of our demonstrating robot's work space. Each object was placed once at each of the positions depicted in Figure 1. The time needed to plan the trajectory and execute the grasp until reaching force closure is listed in Table 2 for each object/position combination. The diagonal of the table represents the actual object/position setup during our experiment.

Table 2: Duration of grasp planning calculation for all object/position combinations in seconds. UL=upper left, LL=lower left, UR=upper right, LR=lower right.

Object position	Object #					
	#1	#2	#3	#4	#5	#6
Left	**33.0**	68.5	11.0	14.1	16.0	24.5
UL	25.5	**34.0**	16.5	13.5	39.0	46.7
LL	11.0	72.6	**11.0**	18.0	22.5	65.0
UR	15.5	42.5	15.0	**12.5**	37.0	46.0
LR	12.0	48.5	11.0	19.0	**22.5**	24.5
Right	11.0	35.6	13.0	14.5	19.5	**29.5**

The results indicate that the duration of grasp planning depends on many parameters. The most important determinant of execution time is the number of point poles ($O(n^2)$) which depends on the level of detail of the object surface as well as the physical constraints of the robot and object position. We observed that even minimal differences in object arrangement appear to have strong influence on force closure termination. This is also indicated by different execution times of identical objects at symmetric positions (e.g. left/right). We consider it likely that these differences are caused by numerical precision issues due to the high number of summations in equations (3) and (4) (see Appendix).

4 DISCUSSION

In the present work we demonstrated that the oddball paradigm is well suited for use in a BCI to reliably select one of several objects for grasping. Importantly, this was achieved independent from eye movements. We demonstrated that the performance of the system improves with training. Furthermore, our results suggest that performance improves even further when subjects obtain more control in the free selection and with realistic visual feedback. This suggests that BCI control in our P300 paradigm is improved with an increasing sense of agency. A gaze independent BCI based on directing covert attention is a fundamental requirement for patients who cannot easily orient gaze to the target object. Earlier reports suggested that eye movements greatly improve performance in a P300 speller (Brunner et al., 2010; Frenzel et al., 2011; Treder and Blankertz, 2010), due to contribution from visual areas to brain wave classification (Bianchi et al., 2010). We extend these previous studies and show that the P300-paradigm is well suited for a gaze independent object grasping BCI. We achieved independence from visual components by instructing our subjects to fixate and by excluding occipital sensors from the analysis. This approach simulates a realistic setting with patients who cannot move their eyes and are therefore dependent on covert attention shift based activation for control. To date, only a small number of studies successfully implemented such a more restrictive covert attention P300 approach (Aloise et al., 2012; Liu et al., 2011; Treder et al., 2011).

We observed increasing decoder accuracy in the course of the experiment. This suggests that the increasing amount of training is beneficial for performance in our BCI paradigm. However, due to classifier updates performed in the course of the experiment, the learning process is likely bilateral and involves both the subjects and the classifier (Curran and Stokes, 2003). Importantly, when subjects were free to select the target object, the decoding success was significantly higher compared to the instructed selections. This suggests a strong role for task involvement and the sense of agency in our paradigm. When subjects performed runs receiving grasp feedback, most of them achieved perfect decoding accuracy. We expect the reliability of the system to be further increased by extending the stimulation interval (Aloise et al., 2012; Hoffmann et al., 2008). Note that system reliability is often more important for the user than a rapid but error prone detection of intention.

The system presented here is efficient for use with nearly no training. Most subjects performed less than ten minutes of training in order to provide data to the decoding algorithm. This is a very small effort compared to motor imagery based systems aiming to control movement in a few degrees of freedom (Hochberg et al., 2012; Wolpaw and

McFarland, 2004).

In online closed-loop BCI studies the decoding algorithm has to be fixed before the start of the actual experiment. We decided to use SVM classification because this is an established classifier for high dimensional feature spaces that provides high and robust generalization by upweighting informative and downweighting uninformative features (Cherkassky and Mulier, 1998). Furthermore, it was shown that linear SVM was equally accurate for P300 detection compared to Fisher's linear discriminant and stepwise linear discriminant analysis (Krusienski et al., 2006). Several existing studies make use of extended linear discriminant analysis algorithms applied to EEG data (Liu et al., 2011; Treder et al., 2011). However, because MEG data are based on a much larger amount of sensors, these approaches are not applicable in a suitable time.

In order to reduce the burden of controlling a complex manipulator with many degrees of freedom by voluntary modulation of brain activity, we combined a P300 BCI with a grasping system that autonomously executes the grasp requiring only a very low input bit rate, namely the command to grasp an object known to the system. To execute the grasp intended by the BCI user, we developed an algorithm for autonomous grasp planning that can place a reliable grasp on natural objects. The execution times we achieved were practical for the proposed task even though not optimal. In this work we did not focus on timing optimization. However, improvements to speed up the calculations are in our focus of future work. The proposed algorithm is universal in the sense that it is not restricted to a specific manipulator. Consequently, this algorithm should also be easily transferable to arbitrary prosthetic devices suitable for grasping potential target objects with a force closure grasp.

As input brain signal for the BCI, we used the MEG. This noninvasive technique measures magnetic fields of cortical dipoles. While the dynamic signal characteristics are comparable to those in EEG, MEG tends to provide higher spatial resolution (Bradshaw et al., 2001). We are aware that this modality is not suitable for daily use and particularly not for use of a prosthetic device. In fact, we consider our study basic research, and to our knowledge, this is the first implementation of a MEG based P300 closed loop BCI.

5 CONCLUSIONS

We showed that noninvasive BCI in combination with an intelligent actuator can be used in real world settings to grasp and manipulate objects. This is an important step towards the development of assistive systems for severely impaired patients.

ACKNOWLEDGEMENTS

This work has been supported by the EU project ECHORD number 231143 from the 7th Framework Programme and by Land-Sachsen-Anhalt Grant MK48-2009/003.

REFERENCES

Aloise, F., Schettini, F., Aricò, P., Salinari, S., Babiloni, F., and Cincotti, F. (2012). A comparison of classification techniques for a gaze-independent P300-based brain-computer interface. *Journal of Neural Engineering,* 9(4), 045012. doi:10.1088/1741-2560/9/4/045012.

Bianchi, L., Sami, S., Hillebrand, A., Fawcett, I. P., Quitadamo, L. R., and Seri, S. (2010). Which physiological components are more suitable for visual ERP based brain-computer interface? A preliminary MEG/EEG study. *Brain Topography* 23(2), 180-185. doi:10.1007/s10548-010-0143-0.

Bradshaw, L. A., Wijesinghe, R. S., and Wikswo, Jr, J. (2001). Spatial filter approach for comparison of the forward and inverse problems of electroencephalography and magnetoencephalography. *Annals of Biomedical Engineering,* 29(3), 214-226. doi:10.1114/1.1352641.

Brunner, P., Joshi, S., Briskin, S., Wolpaw, J. R., Bischof, H., and Schalk, G. (2010). Does the 'P300' speller depend on eye gaze? *Journal of Neural Engineering,* 7(5), 056013. doi:10.1088/1741-2560/7/5/056013.

Cherkassky V. and Mulier, F. (1998). *Learning from Data: Concepts, Theory, and Methods.* John Wiley & Sons.

Curran, E. A. and Stokes, M. J. (2003). Learning to control brain activity: a review of the production and control of EEG components for driving brain-computer interface (BCI) systems. *Brain and Cognition,* 51(3), 326-336. doi:10.1016/S0278-2626(03)00036-8.

Ericson, C. (2005). *Real-time collision detection.* Amsterdam: Elsevier.

Farwell, L. A. and Donchin, E. (1988). Talking off the top of your head: toward a mental prosthesis utilizing event-related brain potentials. *Electroencephalography and Clinical Neurophysiology,* 70(6), 510-523.

Frenzel, S., Neubert, E., and Bandt, C. (2011). Two communication lines in a 3 × 3 matrix speller. *Journal of Neural Engineering,* 8(3), 036021. doi:10.1088/1741-2560/8/3/036021.

Guger, C., Daban, S., Sellers, E., Holzner, C., Krausz, G., Carabalona, R., Gramatica, F., and Edlinger, G. (2009). How many people are able to control a P300-based brain-computer interface (BCI)? *Neuroscience Letters,* 462(1), 94-98. doi:10.1016/j.neulet.2009.06.045.

Guger, C., Edlinger, G., Harkam, W., Niedermayer, I., and Pfurtscheller, G. (2003). How many people are able to operate an EEG-based brain-computer interface (BCI)? *IEEE Transactions on Neural Systems and Rehabilitation Engineering,* 11(2), 145-147. doi:10.1109/TNSRE.2003.814481.

Hochberg, L. R., Bacher, D., Jarosiewicz, B., Masse, N. Y., Simeral, J. D., Vogel, J., Haddadin, S., Liu, J., Cash, S. S., van der Smagt, P., and Donoghue, J. P. (2012). Reach and grasp by people with tetraplegia using a neurally controlled robotic arm. *Nature*, 485(7398), 372-375. doi:10.1038/nature11076.

Hoffmann, U., Vesin, J.-M., Ebrahimi, T., and Diserens, K. (2008). An efficient P300-based brain-computer interface for disabled subjects. *Journal of Neuroscience Methods,* 167(1), 115-125. doi:10.1016/j.jneumeth.2007.03.005.

Khatib, O. (1986). Real-time obstacle avoidance for manipulators and mobile robots. *The International Journal of Robotics Research,* 5(1), 90-98.

Krusienski, D. J., Sellers, E. W., Cabestaing, F., Bayoudh, S., McFarland, D. J., Vaughan, T. M., & Wolpaw, J. R. (2006). A comparison of classification techniques for the P300 speller. *Journal of Neural Engineering*, 3(4). doi: 10.1088/1741-2560/3/4/007.

Kuzborskij, I., Gijsberts, A., and Caputo, B. (2012).On the challenge of classifying 52 hand movements from surface electromyography. *Proceedings of the Annual International Conference of the IEEE Engineering in Medicine and Biology Society (EMBC).* doi:10.1109/EMBC.2012.6347099.

Liu, Y., Zhou, Z., and Hu, D., (2011). Gaze independent brain-computer speller with covert visual search tasks. *Clinical Neurophysiology*, 6. doi:10.1016/j.clinph.2010.10.049.

Pfurtscheller, G., Neuper, C., Guger, C., Harkam, W., Ramoser, H., Schlögl, A., Obermaier, B., and Pregenzer, M. (2000). Current trends in Graz Brain-Computer Interface (BCI) research. *IEEE Transactions on Rehabilitation Engineering,* 8(2), 216-219. doi:10.1109/86.847821.

Quandt, F., Reichert, C., Hinrichs, H., Heinze, H. J., Knight, R. T., and Rieger, J. W. (2012). Single trial discrimination of individual finger movements on one hand: A combined MEG and EEG study. *Neuroimage*, 59(4), 3316-3324. doi:10.1016/j.neuroimage.2011.11.053.

Rieger, J. W., Reichert, C., Gegenfurtner, K. R., Noesselt, T., Braun, C., Heinze, H.-J., Kruse, R., and Hinrichs, H. (2008). Predicting the recognition of natural scenes from single trial MEG recordings of brain activity. *Neuroimage*, 42(3), 1056-1068. doi:10.1016/j.neuroimage.2008.06.014.

Sahbani, A., El-Khoury, S., and Bidaud, P. (2012). An overview of 3D object grasp synthesis algorithms. *Robotics and Autonomous Systems*, 60(3), 326-336. doi:10.1016/j.robot.2011.07.016.

Siciliano, B. and Khatib, O. (2008). *Springer handbook of robotics.* Springer.

Siciliano, B. and Villani, L. (1999). *Robot force control*. Boston: Kluwer Academic.

Treder, M. S. and Blankertz, B. (2010). (C)overt attention and visual speller design in an ERP-based brain-computer interface. *Behavioral Brain Functions,* 6, 28. doi:10.1186/1744-9081-6-28.

Treder, M. S., Schmidt, N. M., and Blankertz, B. (2011). Gaze-independent brain-computer interfaces based on covert attention and feature attention. *Journal of Neural Engineering,* 8(6), 066003. doi:10.1088/1741-2560/8/6/066003.

Velliste, M., Perel, S., Spalding, M. C., Whitford, A. S., and Schwartz, A. B. (2008). Cortical control of a prosthetic arm for self-feeding. *Nature*, 453(7198), 1098-1101. doi:10.1038/nature06996.

Vidaurre, C. and Blankertz, B. (2010). Towards a cure for BCI illiteracy. *Brain Topography,* 23(2), 194-198. doi:10.1007/s10548-009-0121-6.

Wolpaw, J. R. (2013). Brain-computer interfaces. *Handbook of Clinical Neurology 110*, 67-74. doi:10.1016/B978-0-444-52901-5.00006-X.

Wolpaw, J. R., Birbaumer, N., Heetderks, W. J., McFarland, D. J., Peckham, P. H., Schalk, G., Donchin, E., Quatrano, L. A., Robinson, C. J., and Vaughan, T. M. (2000). Brain-computer interface technology: a review of the first international meeting. *IEEE Transactions on Rehabilitation Engineering,* 8(2), 164-173. doi:10.1109/TRE.2000.847807.

Wolpaw, J. R. and McFarland, D. J. (2004). Control of a two-dimensional movement signal by a noninvasive brain-computer interface in humans. *Proceedings of the National Academy of Sciences of the United States of America,* 101(51), 17849-17854. doi:10.1073/pnas.0403504101.

APPENDIX

In section 2.4 we stated the rasterizing of the object and gripper surfaces with virtual point poles. Here we describe the algorithm in more detail.

Our grasp planning algorithm is organized by simulating the action of forces between target object and manipulator in consecutive time frames. While the object poles P^O are defined as positive, the manipulator poles P^M are defined as negative. In accordance with Khatib (1986), we assume that opposite poles attract each other while like poles do

not interact. The magnitude of the force between two poles P_i^O and P_j^M we calculated as

$$\left\|\vec{F}\left(P_i^O, P_j^M\right)\right\| = e^{-\left\|\overrightarrow{P_i^O P_j^M}\right\|} \quad (1)$$

where $\left\|\overrightarrow{P_i^O P_j^M}\right\|$ is the distance between the poles, and the unit of F is arbitrary. The exponential function limits F to a maximum of 1 unit. This avoids infinite forces at collision scenarios and provides a suitable scaling to instantiate both propulsive forces between manipulator and object and repulsive forces to reject manipulator poles that penetrate the object's boundary.

The total propulsive force $\vec{F}(P_i^M)$ affecting one point pole P_i^M on the manipulator is calculated from a set of object point poles A_O where

$$A_O(P_i^M) := \left\{P_j^O \middle| P_j^O \in P^O \wedge \vec{n}_j^O \cdot \vec{n}_i^M < 0\right\} \quad (2)$$

which indicates that only pairwise point poles with an angle between the surface normal $\vec{n}_i^M$ and $\vec{n}_j^O$ greater than $\pi/4$ are involved. We included this constraint to restrict interactions to opposing surface force vectors. The force $\vec{F}(P_i^M)$ that moves the manipulator is then calculated as

$$\vec{F}(P_i^M) = \sum_{P_j^O \in A_O(P_i^M)} \vec{F}\left(P_i^O, P_j^M\right). \quad (3)$$

The manipulator's effective joint torque $\vec{\tau}$ can be calculated by means of the Jacobian J generated from the joint angles $\vec{q}$ and the point poles P^M (Siciliano and Villani, 1999) by

$$\vec{\tau} = \sum_i J(P_i^M, \vec{q})^T \begin{bmatrix} \vec{F}(P_i^M) \\ \vec{M} \end{bmatrix} \quad (4)$$

where external moments are considered $\vec{M} = \vec{0}$. In order to simulate the manipulator movement, we calculated the new joint angle $q_k(t)$ of an axis k by solving the equation system

$$\dot{q}_k(t) = \dot{q}_k(t - \Delta t) + \Delta t * \frac{\tau_k}{\overrightarrow{a_k}^T I(\vec{q}) \overrightarrow{a_k}} \quad (5)$$

$$q_k(t) = q_k(t - \Delta t) + \Delta t * \dot{q}_k(t) \quad (6)$$

where $I(\vec{q})$ is the inertia tensor of the robot's solid elements and $\overrightarrow{a_k}$ defines one of the manipulator axes. We chose a heuristically dynamic calculation of the time frame length Δt which is proportional to the mean distance between the set of point poles P^M and P^O.

Collision detection was performed for the new posture before a new time frame was assigned to be valid and the position update was sent to the manipulator. We used standard techniques (Ericson, 2005) to detect surface intersections. If intersections were detected, repulsive forces were calculated for the affected point poles directing to their position of the last valid time frame and satisfying equation (1). If no intersections were detected, the robot moved to the new coordinates. This procedure was repeated until the force closure condition (Siciliano and Khatib, 2008) was detected.